

Divergent nonlinear response from quasiparticle interactions

Michele Fava,¹ Sarang Gopalakrishnan,^{2,3} Romain Vasseur,⁴ Fabian H.L. Essler,¹ and S. A. Parameswaran¹

¹*Rudolf Peierls Centre for Theoretical Physics, Clarendon Laboratory, Oxford OX1 3PU, UK*

²*Department of Physics, The Pennsylvania State University, University Park, PA 16802, USA*

³*Department of Electrical and Computer Engineering,*

Princeton University, Princeton, New Jersey 08544, USA

⁴*Department of Physics, University of Massachusetts, Amherst, MA 01003, USA*

(Dated: August 23, 2022)

We demonstrate that nonlinear response functions in many-body systems carry a sharp signature of interactions between gapped low-energy quasiparticles. Such interactions are challenging to deduce from linear response measurements. The signature takes the form of a divergent-in-time contribution to the response – linear in the case when quasiparticles propagate ballistically – that is absent for free bosonic excitations. We give an intuitive semiclassical picture of this singular behaviour, validated against exact results from a form-factor expansion of the Ising chain. We discuss extensions of these results to more general settings, finite temperature, and higher dimensions.

Introduction.— The response of a quantum many-body system to external perturbations is central to experimentally extracting information about its properties. In typical settings, such as transport and scattering measurements, the system is weakly perturbed out of its equilibrium state, and the leading linear response [1, 2] contribution can be related via the fluctuation-dissipation theorem to a two-point equilibrium correlation function. Consequently, linear response functions are often relatively straightforward to interpret. For instance, at zero temperature ($T = 0$), as long as the external perturbation can create single quasiparticle (QP) excitations on top of the ground state, their dispersion can be read off directly from momentum-resolved linear-response data. However, the simplicity that lends power to linear response often limits its utility in more complex situations. For example, various distinct physical mechanisms can give rise to a broad frequency spectrum in linear response functions: e.g., selection rules requiring probe fields to excite multiple QPs, inhomogeneous broadening due to quenched disorder or nontrivial dispersion, and homogeneous broadening from QP decay. Differentiating among these using linear response data alone is a challenge, further heightened when momentum resolution is absent, as in optical probes which typically give a spatially-averaged (“ $q = 0$ ”) snapshot of the system under study.

Often, nonlinear response functions give more direct insight into the nature of the low-energy excitation spectrum [3]. Intuitively, this is because they involve multi-time correlation functions that, suitably analysed, can disentangle different sources of broad spectra [4]. Pump-probe experiments [5, 6] and two-dimensional coherent spectroscopy (2DCS) [7–12] both extract nonlinear response functions. They have long been used in magnetic resonance and optical experiments on chemical systems, usually in regimes where the response reduces to that of individual atoms, averaged over a suitable statistical ensemble. The extended many-body systems usually encountered in solid-state materials or ultracold atomic

gases do not always admit a similarly simplified description. Developing techniques to compute nonlinear response functions in such systems is thus an important goal [13–24], made more pressing as experiments begin to probe such regimes. Apart from situations that reduce to an ensemble of few-body systems [4, 25, 26], most controlled results have been obtained from free theories [4, 27–30], or exactly-solvable models [31–36]. There is thus a need for qualitative insights into universal aspects of nonlinear response outside these settings.

Here, we offer such a qualitative perspective: a semiclassical theory of nonlinear response. We focus on the simplest non-trivial systems, whose low-energy spectrum consists of gapped QPs and where the perturbing field can excite single QPs. For ballistic QPs in one dimension ($d = 1$) and at $T = 0$ we find that the $q = 0$ third-order response functions diverge linearly in the time interval between distinct applications of the external field, with a strength set by the inter-QP scattering phase shifts, and a scaling function specific to the nonlinear protocol. This richness is to be contrasted with $q = 0$ linear response for such systems: a delta-function peak at the gap frequency whose strength is related to the stability of QPs, and is nonzero even for free bosonic QPs with no scattering.

Apart from enjoying the simplifying features of ballistic $d = 1$ QPs, the primary example we consider below – the transverse-field Ising chain – is also integrable. As is well known, it maps to a theory of free fermionic QPs, whose statistics enforce a scattering phase shift of -1 leading to singular nonlinear response. We benchmark semiclassical analysis for the Ising model against exact results using form-factor expansions, detailed in upcoming work [37]. While the form-factor approach is applicable to a subset of integrable models, the semiclassical approach can be generalized more broadly: with only slightly more work, we can treat [low] finite T and non-integrable systems, as long as the system hosts gapped QPs with a well-defined dispersion. We also conjecture that many features persist in $d > 1$. Relaxing the re-

striction to $q = 0$ to allow momentum resolution permits direct extraction of the QP scattering matrix by combining linear and nonlinear response data. Our work thus promises an intuitive way to compute nonlinear responses in a variety of quantum many-body systems.

Setup.—As noted above, we initially focus on the transverse field Ising chain, with Hamiltonian

$$H = -J \sum_{j=0}^{L-1} (\sigma_j^z \sigma_{j+1}^z + g \sigma_j^x). \quad (1)$$

In particular, we work in the paramagnetic phase ($g > 1$) and consider $q = 0$ perturbations coupling to the order parameter $M = \sum_j \sigma_j^z$ (recall that only such ‘Ising-odd’ operators can excite single QPs above the ground state).

The model is exactly solvable by means of a Jordan-Wigner transformation [38] that maps eq. (1) to a quadratic (free) fermion problem. This yields a QP dispersion relation $\epsilon(k) = 2J\sqrt{1 + g^2 - 2g \cos(k)}$, with a gap $\Delta = \epsilon(0)$. Note that, although H maps to free fermions, σ^z maps to a non-local (string-like) operator. Therefore, exact response functions involving M cannot be easily computed using free-fermion methods e.g. Wick’s theorem, and instead require a form-factor expansion using techniques developed in Refs [38–46]. Similarly, any local spin operator that can create single fermionic QPs must be nonlocal in the fermion basis. Consequently, their nonlinear response is sharply distinct from that of fermion-local spin observables [4], that only excite even numbers of QPs.

We first study the pump-probe signal,

$$\Xi_{\text{PP}} = -\frac{i}{L} \langle 0 | e^{i\mu M(0)} [M(t_1 + t_2), M(t_1)] e^{-i\mu M(0)} | 0 \rangle + \frac{i}{L} \langle 0 | [M(t_2), M(0)] | 0 \rangle, \quad (2)$$

which can be viewed as the difference in the linear response (measured between times $t_1, t_1 + t_2$) computed in two states: the original QP vacuum $|0\rangle$, and a ‘pumped’ state $e^{-i\mu M(0)} |0\rangle$ obtained by perturbing the QP vacuum at $t = 0$ with a ‘kick’ of strength μ coupling to M .

In the response regime where the pump only weakly perturbs the system away from equilibrium, we can expand Ξ_{PP} in μ and evaluate the resulting correlators in equilibrium: odd powers vanish by symmetry, so $\Xi_{\text{PP}} = \mu^2 \chi_{\text{PP}}^{(3)} + O(\mu^4)$. The superscript denotes a third-order response, which we split into pieces divergent and convergent in time, $\chi_{\text{PP}}^{(3)} = \chi_{\text{PP};d}^{(3)} + \chi_{\text{PP};c}^{(3)}$, where the former

$$\chi_{\text{PP};d}^{(3)} = \frac{2}{L} \Im \langle 0 | M(0) M(t_1 + t_2) M(t_1) M(0) | 0 \rangle_C \quad (3) \\ = \frac{2}{L} \Im \langle 0 | \underbrace{M e^{iH(t_1+t_2)} M e^{-iHt_2}}_{\text{bra}} \underbrace{M e^{-iHt_1} M}_{\text{ket}} | 0 \rangle_C,$$

is our focus. Only the connected correlator (denoted by the subscript C) contributes to the response, as required

by causality. We have written eqs. (2) and (3) in the Heisenberg picture; evidently they are not time-ordered. It is convenient to also distinguish the ‘ket’ and ‘bra’ sides of eq. (3) viewed in the Schrödinger picture. Formally these correspond to forward and backward branches of the Keldysh time contour, which runs from $t = 0$ to $t = t_1 + t_2$ and back. At $t = 0$, the operator M acts on bra and ket sides, whereas at time $t = t_1$ it acts solely on the ket side. Both sides are then evolved up to time $t = t_1 + t_2$, whereupon M is measured. This sequence is path-ordered on the Keldysh contour, in contrast to out-of-time-order correlators studied in quantum chaos [47–49]. We adopt the standard nomenclature where n^{th} order response functions involve n external fields and $n + 1$ operators; the extra operator corresponds to the measured observable. [More properly, $\chi_{\text{PP}}^{(3)}$ involves another field μ' and hence scales as $\mu^2 \mu'$. μ' is required to extract the linear response in the pumped state.]

Long-time divergences and non-perturbative effects.—Our main result is that $\chi_{\text{PP};d}^{(3)}$ diverges at late times,

$$\chi_{\text{PP};d}^{(3)} \simeq 2 \sin(\Delta t_2) (t_1 + t_2) \mathcal{C}_{\text{PP}} \left(\frac{t_2}{t_1 + t_2} \right) \quad (4)$$

with a scaling function \mathcal{C}_{PP} whose numerical behaviour is shown in Fig. 2. This divergence can be given a simple semiclassical interpretation, involving ballistic propagation of quasiparticles and their scattering (Fig. 1).

Before detailing the semiclassical analysis, we argue that we expect $\chi_{\text{PP}}^{(3)}$ to diverge on general grounds. Even for arbitrarily small perturbation strength μ , Ξ_{PP} will saturate to an $O(1)$ value independent of μ at late times. This is most easily seen for sufficiently large t_1 , such that the system effectively thermalizes after the initial kick. The perturbed state $e^{-i\mu M(0)} |0\rangle$ is then effectively at a finite (but small) T . [In the integrable case, it can be approximated by a generalized Gibbs ensemble (GGE) (see Appendix), but this is not essential to the analysis.] The first line of eq. (2) is then approximately a linear-response function in a finite- T state, which on general grounds is expected to decay exponentially with dephasing rate γ_μ ,

$$\langle e^{i\mu M(0)} [M(t_1 + t_2), M(t_1)] e^{-i\mu M(0)} \rangle \sim e^{-\gamma_\mu t_2}, \quad (5)$$

intuitively due to stochastic scattering events with the QPs created by $e^{-i\mu M(0)}$ [50]. Thus eq. (2) becomes a difference of correlators at finite and zero T , and as the latter exhibits undamped oscillations in time we have $\Xi_{\text{PP}} \sim O(\mu^0)$. On the other hand, expanding (2) in a power series in μ (at large, finite L) gives $\Xi_{\text{PP}} = \sum_{n \geq 2} \mu^{2n} g_{2n}(t_1, t_2)$. This can only become $O(\mu^0)$ at late times $t_{1,2}$ if the expansion is not uniformly convergent. A natural possibility is to have an ‘infrared divergence’ that needs to be summed to all orders in μ . In the Ising case we expect exponentiation of the dominant contribution in the late-time regime, so that

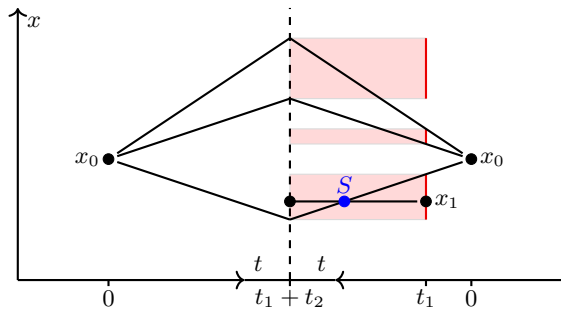


FIG. 1. Cartoon of processes contributing to the late-time divergence of the third-order response $\chi_{PP;d}^{(3)} \sim \langle M(0)M(t_1+t_2)M(t_1)M(0) \rangle$. A dashed line, corresponding to time $t = t_1+t_2$ separates the bra (left) and ket (right) sides of the time evolution; time increases towards this line. Solid lines denote QP worldlines, and circles denote the action of the operator M . When two lines cross, the amplitude for the diagram is multiplied by $S = -1$. For a fixed x_0 , the red segments indicate the set of x_1 giving rise to a scattering-connected contribution. The length of the red set is proportional to the overall timescale, leading to the linear divergence in Eq. (4).

$\Xi_{PP} \sim (1 - e^{-c\mu^2 t_2}) \langle 0 | [M(t_2)M(0)] | 0 \rangle$. These considerations suggest that $\chi_{PP}^{(3)}$ diverges whenever we have a stable QP excitation at zero momentum, which gets damped at finite energy densities. Thus the nonlinear response initially shows a linear divergence, probed in the response limit, that eventually saturates at late times $t \gg 1/\mu^2$.

Semiclassical picture.—The scaling form eq. (4) and the scaling function \mathcal{C}_{PP} can be quantitatively understood from a simple semiclassical picture inspired by the seminal approach of Refs. 50 and 51 (see also Refs. 52–55). Our basic objects are wave-packet (WP) states $|r, k\rangle$ of QPs, which we will think of as having approximately well-defined positions r and momenta k in the sense that the effects of the dispersion of the wave packets will be sub-leading. Multi-WP states $|\mathbf{r}; \mathbf{k}\rangle$ are obtained as tensor products of single-WP states and by locality of the Hamiltonian (approximately) have simple dynamics as long as the WPs are spatially well separated. By construction n -WP states are in one-to-one correspondence with scattering states of n QPs. On the ket side, the action of the operator $M(0)$ will after a sufficiently long time result in “intermediate” n -WP states (with n odd), where the individual WPs approximately originate from the same point x_0 (which is integrated over) and whose momenta sum to 0. Each WP (approximately) propagates ballistically with its group velocity $v(k) = \epsilon'(k)$, i.e. $e^{-iHt}M(0)|0\rangle$ is approximately a superposition of states of the form $\int dx_0 |\mathbf{r}; \mathbf{k}\rangle$ with \mathbf{r} specified by $r_j = x_0 + v(k_j)t$ and \mathbf{k} such that $\sum_j k_j \approx 0$, but otherwise arbitrary. We start by considering processes where all WPs proceed undisturbed to time t_1+t_2 , whereupon they annihilate with the n WPs produced by $M(0)$ on the bra side. Note that, in order to have a non-negligible

overlap between the bra and the ket, the momenta \mathbf{k} on the two sides must approximately coincide, as well as the position x_0 at which the WP shower is created (see Fig. 1). In the Ising model the amplitude associated with creating and annihilating a shower of n WPs with a given set of momenta \mathbf{k} is $|F_n(\mathbf{k})|^2 \frac{d^n \mathbf{k}}{(2\pi)^{n-1}} \delta\left(\sum_{j=1}^n k_j\right)$ for every initial position x_0 . Here $F_n(\mathbf{k}) = \langle \mathbf{k} | \sigma_0^z | 0 \rangle$ is the so-called n -QP form factor on top of the ground state, whose precise value is unnecessary to proceed with the semiclassical calculation.

In the processes of interest, $M(t_1)$ creates a single $q = 0$ WP at x_1 , which is spatially well separated from the position at time t_1 of the n WPs produced by the action of $M(0)$ on $|0\rangle$. The WP created by $M(t_1)$ is then annihilated by $M(t_1+t_2)$, giving rise to an amplitude $|F_1(0)|^2 e^{-i\Delta t_2}$. Naively, integrating over the arbitrary positions x_0 and x_1 generates a contribution to $\chi_{PP}^{(3)}$ that diverges proportionally to L in the thermodynamic limit. However, the contribution of processes in which the WP trajectories do not cross is simply equal to the product of two-point functions $L^{-1} \langle M(0)M(0) \rangle \langle M(t_1+t_2)M(t_1) \rangle$, and therefore the extensive spatial divergence cancels when we subtract the disconnected contributions.

In contrast, each time a pair of WP trajectories cross, the amplitude for the process picks up a factor of the scattering matrix S . In the Ising model, this simply encodes the fermionic statistics of QPs, i.e. $S = -1$. Therefore, a process involving an odd number of scattering events (cf. Fig. 1) does not cancel against disconnected contributions; we refer to processes which are connected only because of such events as *scattering-connected*. After subtracting the disconnected component we obtain a factor $S - 1$, evaluating to -2 in the Ising case. Finally, we must integrate over all possible x_1 that produce a scattering-connected process. [The integration over x_0 will produce a factor L , cancelling the L^{-1} in the definition of $\Xi_{PP}^{(3)}$.] One can verify that, for a given set of momenta \mathbf{k} of the WPs produced by the pump, the range of x_1 leading to scattering-connected processes has length $v_{PP}(t_1+t_2)$, where v_{PP} has the dimension of a velocity and is obtained as follows: we define the set of positions $Y = \{v(k_1)t_1, \dots, v(k_n)t_1, v(k_1)(t_1+t_2), \dots, v(k_n)(t_1+t_2)\}$ and then reorder the elements $y_j \in Y$ such that $y_1 < y_2 < \dots < y_{2n}$. Then $v_{PP}(\mathbf{k}) = \frac{1}{t_1+t_2} \sum_{j=1}^{2n} (-1)^j y_j$. In this way we obtain a divergent contribution to $\chi_{PP;d}^{(3)}$ of the form (4) with $\mathcal{C}_{PP} = 4\pi \sum_{n,\text{odd}} \mathcal{C}_{PP}^{(n)}$, where

$$\mathcal{C}_{PP}^{(n)} = -\frac{|F_1(0)|^2}{n!} \int \frac{d^n \mathbf{k}}{(2\pi)^n} \delta\left(\sum_{j=1}^n k_j\right) |F_n(\mathbf{k})|^2 v_{PP}(\mathbf{k}). \quad (6)$$

Note that for $g \gtrsim 1.1$, \mathcal{C}_{PP} is dominated by $\mathcal{C}_{PP}^{(3)}$, with higher values of n yielding numerically smaller corrections. This allows us to numerically estimate \mathcal{C}_{PP} , reported in Fig. 2 for representative values of g .

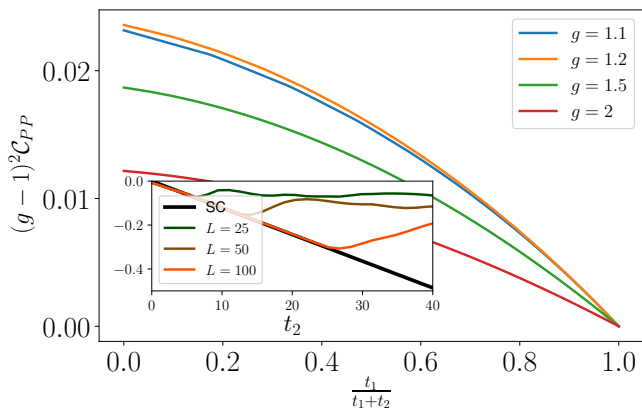


FIG. 2. Scaling function $\mathcal{C}_{PP}(\frac{t_1}{t_1+t_2})$ as defined in Eq. (4) for various values of the transverse field g and $J = 1$. In order to show the results at various g within the same plot, \mathcal{C}_{PP} has been rescaled by $(g-1)^2$. Inset: $\chi_{PP;3,4,3}^{(3)}/(2\sin(\Delta t_2))$ as a function of t_2 for $t_1 = 0$, $g = 2$, and $J = 1$. Various coloured curves denote the exact results obtained by numerically summing the form factors in an L -sites chain. The black line gives the linear scaling due to $\mathcal{C}_{PP,3}$ computed through the semiclassical formula in Eq. (6).

Other types of processes only give rise to subleading contributions at late times. Scattering-connected processes where $M(t_1)$ creates more than one QP subsequently annihilated by $M(t_1+t_2)$ give contributions suppressed as $t_2 \rightarrow \infty$. This follows since QPs created by $M(t_1)$ spread ballistically from one another and therefore cannot be annihilated by a single local operator. For processes that are not simply scattering-connected, the position where all operators act is fixed by the ballistic propagation of the various QPs, therefore we expect their contributions to remain finite at late times.

Form-factor expansion.— We bolster the semiclassical result with an exact calculation of the late-time asymptotics of $\chi_{PP;d}^{(3)}$ via a form-factor expansion [38–46]. Inserting resolutions of the identity in terms of energy eigenstates between each pair of operators yields

$$\chi_{PP;d}^{(3)} = \sum_{n_a, n_b, n_c} \chi_{PP;d}^{(3), [n_a, n_b, n_c]}, \quad (7)$$

where $\chi_{PP;d}^{(3), [n_a, n_b, n_c]}$ denotes terms that have the form $\langle 0|M|\mathbf{K}\rangle \langle \mathbf{K}|M|\mathbf{p}\rangle \langle \mathbf{p}|M|\mathbf{k}\rangle \langle \mathbf{k}|M|0\rangle$. Here \mathbf{K} , \mathbf{p} , and \mathbf{k} label the sets of momenta of the n_a , n_b and n_c QPs in the eigenstate. M couples only the odd-QP [Ramond] sector to the even-QP [Neveu-Schwarz] sector. Consequently, n_a and n_c are odd, while n_b is even, so the momenta in \mathbf{p} and $\{\mathbf{K}, \mathbf{k}\}$ must be compatible with anti-periodic and periodic boundary conditions, respectively.

A key property of the Ising form factors [56–59] is the kinematic pole in matrix elements of M : as an outgoing momentum p_i approaches an incoming momentum k_j , $\langle \mathbf{p}|M|\mathbf{k}\rangle \sim \frac{1}{p_i - k_j}$. [Note that since the $|p_i - k_j| \gtrsim L^{-1}$

due to the different boundary conditions, the $\langle \mathbf{p}|M|\mathbf{k}\rangle$ are finite for any finite L .] These poles ultimately generate the late-time divergence within the form-factor approach.

To benchmark the semiclassical picture, we consider its simplest non-zero contribution, from $\mathcal{C}_{PP}^{(3)}$ (sketched in Fig. 1). Counting the number of QPs before and after each operator M , we expect that $\mathcal{C}_{PP}^{(3)}$ is linked to $\chi_{PP;d}^{(3);[3,4,3]}$ in the form-factor expansion. Numerically evaluating $\chi_{PP;d}^{(3);[3,4,3]}$ we see good agreement with the semiclassical expectation (see inset of Fig. 2).

We can also use the form-factor approach to compute the leading correction to eq. (4), which scales as $\sqrt{t_2}$ [60, 61]. We conjecture that this can be interpreted as the effect of scattering-connected processes where $M(0)$ and $M(t_1+t_2)$ create and annihilate a single QP, which can scatter with the QP being exchanged between $A(t_1)$ and $A(t_1+t_2)$ when their trajectories are smeared by the broadening of QP wavepackets due to dispersion, omitted in the leading semiclassical analysis.

2DCS.— Similar conclusions apply to 2DCS experiments, where the system is perturbed by a pair of field pulses at varying times. The corresponding third-order response, usually analysed in a ‘two-frequency plane’ is expressible in terms of the subset of 4-point correlators that have exactly one pair of coincident times. At late times, the leading third-order 2DCS contribution is the sum of a pump-probe response in Eq. (4), and the so-called ‘non-rephasing’ signal

$$\chi_{NR;d}^{(3)} = \frac{2}{L} \Im \langle M(t_1)M(t_1+t_2)M(t_1)M(0) \rangle_C. \quad (8)$$

$\chi_{NR;d}^{(3)}$ has an almost identical structure to $\chi_{PP;d}^{(3)}$; its leading processes are those where a shower of n QPs are exchanged between the two copies of $M(t_1)$, and a single QP is exchanged between $M(0)$ and $M(t_1+t_2)$. Proceeding similarly to the pump-probe case, we find

$$\chi_{NR;d}^{(3)} \simeq 2 \sin[\Delta(t_1+t_2)] t_2 v_{NR}, \quad (9)$$

where $v_{NR} = \mathcal{C}_{PP}(0)$ has the dimension of a velocity.

In the two-frequency space our findings translate into pronounced singularities. This is most easily understood for $\chi_{NR;d}^{(3)}$, which would produce a singularity near the point $(\omega_1, \omega_2) = (\Delta, \Delta)$ of the form $[(\omega_1 - \Delta) + i0^+]^{-1} \partial_{\omega_2} [(\omega_2 - \Delta) + i0^+]^{-1}$. Here ω_1 and ω_2 denote the frequency associated to t_1 and t_2 respectively. A similar, albeit more complex, structure emerges around the point $(\omega_1, \omega_2) = (0, \Delta)$ due to $\chi_{PP;d}^{(3)}$. Nonetheless, we believe the long-time divergences should be most convenient to diagnose directly in real time.

Low-temperature regime.— In the case of the Ising model the semiclassical picture above can be extended to study the low-temperature regime, i.e. $k_B T \ll \Delta$. As in Ref. 50, we approximate the thermal density matrix as a diagonal ensemble of WP states, i.e. WPs representing

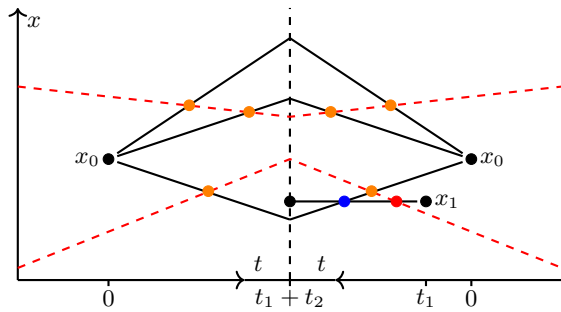


FIG. 3. Cartoon of low temperature semiclassical processes. The thermal state is approximated as an ensemble of WP states representing thermal QPs, which follow the same trajectories on bra and ket sides (dashed red lines). As they propagate, the thermal QPs can scatter against those produced by $M(0)$ (orange dots) and by $M(t_1)$ (red dot). Each orange dot on the bra side is canceled by its partner on the ket side, and hence they do not affect the amplitude. This reduces the problem in essence to that solved in Ref. 50.

thermal QPs run on both bra and ket branches with identical trajectories, and affect the response solely via their purely elastic scattering with the QPs created by the M operators. As depicted in Fig. 3, thermal QPs will scatter both against those produced by $M(t_1)$ (red dot), and those produced by the pump (orange dots). Crucially, since the trajectories of both thermal and pumped QPs are identical on bra and ket sides, the latter scattering processes always cancel out and hence do not alter the correlator. In contrast, each time a thermal QP scatters with a QP singularly produced at x_1 the amplitude of the process acquires a factor $S = -1$. Since the amplitude now fluctuates depending on the number of thermal QPs encountered, averaging over the distribution of the latter results in an exponential decay of the signal controlled by the dephasing rate [50] $\gamma_T \simeq \frac{2k_B T}{\pi} e^{-\Delta/k_B T}$. Therefore the finite- T pump-probe and non-rephasing signals are asymptotically given by

$$\begin{aligned} \chi_{\text{PP};d}^{(3)}(T > 0) &\simeq \chi_{\text{PP}}^{(3)}(T = 0) e^{-\gamma_T t_2} \\ \chi_{\text{NR}}^{(3)}(T > 0) &\simeq \chi_{\text{NR}}^{(3)}(T = 0) e^{-\gamma_T(t_1+t_2)}. \end{aligned} \quad (10)$$

[A possibly more accurate estimate might be to replace $|F_1(0)|^2 \sin(\Delta \dots)$ with the finite-temperature two-point function [39–42, 46, 62].] The divergence is thus cut off at $t^* \sim e^{\Delta/k_B T}$, and is observable if $k_B T \lesssim \Delta$.

Discussion.—We have shown that in the transverse-field Ising model the nonlinear pump-probe response is characterised by a linear-in-time divergence. We will now argue that this is in fact a general feature of any interacting translationally-invariant many-body system that has a stable, gapped single-particle excitation. Such a behaviour is suggested by our analysis where we demonstrated that the late-time pump-probe signal Ξ_{PP} can be re-expressed as the difference of two-point correlation functions at zero and finite temperatures and hence is

$O(1)$; the divergent response reconciles this result with the perturbative expansion in powers of the applied fields. We therefore expect this linear-in-time growth to be quite general and as we have argued, in many cases visible also on intermediate timescales at low finite temperature. We have developed a semiclassical picture of WP propagation and scattering that identifies the processes that give rise to the divergence. Our discussion has focused on the simple case of the Ising model, which is special as it is both integrable and maps onto a free theory. However, the form factor calculations in fact generalize to interacting integrable theories as is shown in a forthcoming work [37]. More importantly, the semiclassical arguments generalize to non-integrable models [37].

An enticing possibility suggested by our work is the measurement of scattering matrices from third-order response functions. For this, we require at least 2 of the 4 M s in the correlator to be at finite momentum q . This could for example be achieved by measuring linear response in a $q = 0$ pumped state via a momentum-resolved probe. Furthermore, we also need to work in a regime where the $n = 1$ contribution dominates \mathcal{C}_{PP} . This is automatic when the gap is large, but can also be achieved using a frequency-modulated pump with negligible amplitude to excite the system at energies greater than 2Δ . In such settings, we find

$$\begin{aligned} \chi_{\text{PP};d}^{(3)} &\simeq 2i \frac{\langle M(0,0)M(0,0) \rangle}{L} \frac{\langle M(-q,t_1+t_2)M(q,t_1) \rangle}{L} \\ &\times (S(|q|,0) - 1) |v(q) - v(0)| t_2 + \text{c.c.} \end{aligned} \quad (11)$$

with $S(|q|,0)$ denoting the forward scattering amplitude between a QP with momentum $|q|$ and one with momentum 0. Crucially, every term except $S(|q|,0)$ in this expression can be extracted from linear response, allowing us to read off $S(|q|,0)$ from the divergent piece of $\chi_{\text{PP}}^{(3)}$.

Finally, it would be interesting to understand if similar late-time divergences emerge in $d > 1$. The non-perturbative argument is evidently independent of dimension, suggesting that this is indeed the case. Thinking semiclassically and considering third-order response at finite momentum q , as defined above, processes where each operator produces or annihilates a single QP could lead to a divergence proportional to t_2 . Even in this case, once all impact parameters are fixed, there is still a single degree of freedom which is arbitrary in the semiclassical picture: the time $t_S \in [t_1, t_1 + t_2]$ at which the scattering occurs. Crucially, the scattering amplitude must be t_S -independent, so after integrating over all positions, this gives a contribution proportional to t_2 . We leave a more detailed investigation of this intriguing possibility to future work. It would be interesting to understand if these or similar mechanisms are responsible for the anomalously large nonlinear response recently observed in 2DCS experiments [12].

Acknowledgments.—We thank Abhishodh Prakash, Nick Bultinck and especially Sounak Biswas for many

insightful discussions. We also thank Sounak Biswas and Max McGinley for collaboration on related projects and Max McGinley for useful comments on the manuscript. We acknowledge support from the European Research Council under the European Union Horizon 2020 Research and Innovation Programme, Grant Agreement No. 804213-TMCS (M.F., S.A.P.), the UK Engineering and Physical Sciences Research Council via Grant No. EP/S020527/1 (F.H.L.E.), the US National Science Foundation under Award No. DMR-1653271 (S.G.), the US Department of Energy, Office of Science, Basic Energy Sciences, under Early Career Award No. DE-SC0019168 (R.V.), and the Alfred P. Sloan Foundation through a Sloan Research Fellowship (R.V.). Statement of compliance with EPSRC policy framework on research data: This publication is theoretical work that does not require supporting research data.

Appendix: Perturbative expansion of Ξ_{PP}

In this appendix we expand Ξ_{PP} , as defined in Eq. (2) to leading order in μ to finally arrive at the definition of $\chi_{\text{PP};d}^{(3)}$ in Eq. (3). We begin by writing

$$\begin{aligned} \Xi_{\text{PP}} &= -i\frac{\mu^2}{L} \langle 0 | M(0)[M(t_1 + t_2), M(t_1)]M(0) | 0 \rangle \\ &\quad + i\frac{\mu^2}{2L} \langle 0 | \left\{ (M(0))^2, [M(t_1 + t_2), M(t_1)] \right\} | 0 \rangle \\ &\quad + O(\mu^3). \end{aligned} \quad (12)$$

Here the zero-order term of the first line of Eq. (2) cancels with the second line, the first-order contribution vanishes because of the \mathbb{Z}_2 symmetry of the Ising model, and $\{\cdot, \cdot\}$ denotes an anticommutator.

The term in the first line is related to $\chi_{\text{PP};d}^{(3)}$ by the addition of the disconnected component

$$\begin{aligned} &-\frac{i}{L} \langle 0 | M(0)[M(t_1 + t_2), M(t_1)]M(0) | 0 \rangle = \\ &= \chi_{\text{PP};d}^{(3)} + \\ &\quad + 2 \langle 0 | M(0)M(0) | 0 \rangle \Im \langle 0 | M(t_1 + t_2)M(t_1) | 0 \rangle. \end{aligned} \quad (13)$$

[Note that other possible ways of breaking the four-point function into a product of two-point functions cancel because of the commutator between $M(t_1 + t_2)$ and $M(t_1)$.] Similarly, defining

$$\chi_{\text{PP};c}^{(3)} = \frac{i}{2L} \langle 0 | \left\{ (M(0))^2, [M(t_1 + t_2), M(t_1)] \right\} | 0 \rangle_C, \quad (14)$$

we have

$$\begin{aligned} &\frac{i}{2L} \langle 0 | \left\{ (M(0))^2, [M(t_1 + t_2), M(t_1)] \right\} | 0 \rangle = \\ &= \chi_{\text{PP};c}^{(3)} + \\ &\quad - 2 \langle 0 | M(0)M(0) | 0 \rangle \Im \langle 0 | M(t_1 + t_2)M(t_1) | 0 \rangle. \end{aligned} \quad (15)$$

Combining these results, we finally arrive at the expression quoted in the main text,

$$\chi_{\text{PP}}^{(3)} = \chi_{\text{PP};d}^{(3)} + \chi_{\text{PP};c}^{(3)}. \quad (16)$$

Appendix: Long-time divergences and non-perturbative effects in integrable systems

In this appendix we further elaborate on the connection between long-time divergences and non-perturbative effects in integrable systems, where the argument can be presented in a more controlled fashion.

As in the main text, we work in the limit of large t_1 , when we can assume that the density matrix can be approximated by a generalized Gibbs ensemble (GGE), i.e. the density matrix takes the form $\rho \sim \exp(-\sum_k \lambda_k n_k)$, obtained by maximizing entropy subject to the conservation of the number of QPs n_k in mode k . Here the λ_k could in principle be fixed by imposing $\langle n_k \rangle = \langle 0 | e^{i\mu M} n_k e^{-i\mu M} | 0 \rangle$ in the GGE. The first line of eq. (2) is then a linear-response function on top of ρ . Given that ρ is a finite energy-density state, this is known to decay exponentially [46].

Appendix: Semiclassical picture as wavepacket kinematics

In this appendix we explain how the semiclassical picture can be made more precise in terms of wavepackets of QPs.

The starting point is the definition of single-QP wavepacket states in terms of asymptotic scattering states:

$$|r, k\rangle = \int \frac{dp}{2\pi} \tilde{W}(p; r, k) |p\rangle \quad (17)$$

$$\tilde{W}(p; r, k) = \exp\left(-\ell^2 \frac{(p-k)^2}{2}\right) e^{i(k-p)r}. \quad (18)$$

Here ℓ is some arbitrary microscopic distance, which we assume to satisfy $\ell \gg \xi$. The evolution of a wavepacket state is simply given by

$$U(t) |r, k\rangle \simeq e^{-i\epsilon(k)t} |r + v(k)t, k\rangle \quad (19)$$

up to corrections which can be neglected by choosing ℓ s.t. $\ell \gg \sqrt{\epsilon''(k)}(t_1 + t_2)$.

Similarly, one can define wavepacket states in terms of asymptotic scattering states as

$$|\mathbf{r}, \mathbf{k}\rangle = \int \frac{d^n \mathbf{p}}{(2\pi)^n} \left(\prod_{j=1}^n \tilde{W}(p_j; r_j, k_j) \right) |\mathbf{p}\rangle. \quad (20)$$

Their time evolution will generally be complicated, however it simplifies in the asymptotic region, i.e. when $|r_i - r_j| \gg \ell \forall i, j$. In this case, each r_j coordinate will evolve ballistically with the group velocity $v(k_j)$. Furthermore, whenever two wavepackets come in proximity of each other, they will scatter. In 1D and for systems with only one QP species, this will amount to the wavefunction acquiring an overall extra phase: the scattering matrix.

Appendix: Semiclassical picture for non-integrable models

We now detail how the wavepacket description above can be used to naturally extend the analysis in the main text to non-integrable models.

The starting point is characterizing the state $M|0\rangle$. In non-integrable systems this state will generally be complicated since M can create multiple excitations in the neighborhood of the same point. After some time t , however, we expect asymptotic QP states to emerge. In this case we can write

$$e^{-iHt} M(0)|0\rangle \simeq \sum_n \frac{1}{\sqrt{n!}} \int dx_0 \int \frac{d^n \mathbf{k}}{(2\pi)^n} e^{-ix_0 \sum_j k_j} \times \mathcal{F}_n(\mathbf{k}) e^{-i \sum_j \epsilon(k_j)t} |\mathbf{r}; \mathbf{k}\rangle \quad (21)$$

with \mathbf{r} specified by $r_j = x_0 + v(k_j)t$. Importantly, for a fixed \mathbf{k} , the integral over y is negligible, unless $|\sum_j k_j| \lesssim \ell^{-1}$. Here \mathcal{F} denotes the probability amplitude to produce a given wave-packet state, and is generally challenging to compute from first principles. Note that in this appendix, the “ \simeq ” sign between two states should not be intended in the sense that the difference between the two has a small norm, but rather that we are isolating a component of the state that will ultimately give the leading contribution to $\chi_{\text{PP};d}^{(3)}$.

The validity of equation above can be argued as follows. In fact, Eq. (21) is not the most general form for a WP state, which would instead be

$$e^{-iHt} M(0)|0\rangle = \sum_n \frac{1}{\sqrt{n!}} \int d^n \mathbf{x} \int \frac{d^n \mathbf{k}}{(2\pi)^{n-1}} \times \mathcal{F}'_n(\mathbf{k}, \mathbf{x}_j) e^{-i \sum_j \epsilon(k_j)t} |\mathbf{r}; \mathbf{k}\rangle \quad (22)$$

with $r_j = x_j + v(k_j)t$. [Note that through the discussion in the previous section we have already ruled out the possibility that \mathcal{F} might contain some additional time

dependence.] Here the initial positions x_j must necessarily be close: i.e. $|x_i - x_j| \lesssim \xi_A$ for some microscopic length ξ_A . However, since we are interested in divergences originating at large lengthscales and timescales, we can choose $\ell \gg \xi_A$, so that we can approximate $x_j \simeq x_0$ for all j and $\mathcal{F}'_n(\mathbf{k}, \mathbf{x}_j) \simeq \mathcal{F}'_n(\mathbf{k}, x_0)$. Finally, the fact that the left-hand side is invariant under translation by any length a requires the x_0 -dependence of $\mathcal{F}'_n(\mathbf{k}, x_0 + a) e^{ia \sum_j k_j} = \mathcal{F}'_n(\mathbf{k}, x_0)$, implying that $\mathcal{F}'_n(\mathbf{k}, x_0)$ is of the form $e^{-ix_0 \sum_j k_j} \mathcal{F}_n(\mathbf{k})$.

Finally, for the semiclassical analysis of the divergence we also need to use that

$$M|\mathbf{r}, \mathbf{n}\rangle = \int_{\text{asymptotic region}} dr' F_1(0) |(\mathbf{r}, r'); (\mathbf{k}, 0)\rangle + \sum_j F_1^*(0) |(r_1, \dots, \cancel{r_j}, \dots, r_n, r'); (k_1, \dots, \cancel{k_j}, \dots, k_n, 0)\rangle + \dots \quad (23)$$

Here the first term amounts to adding a zero-momentum WP at position r' , which is possible if $|r' - r_j| \gg \ell$ for all j . The second line accounts for processes where M annihilates one of the previously-present WPs, instead. Finally, the \dots denote more complicated outcomes, e.g., where more than one WP is created or annihilated.

We can now discuss in detail the bra and ket side of Eq. (3). The bra side can be simply expanded as in Eq. (21)

$$\langle \psi_4 | = \langle 0 | M(0) e^{+iH(t_1+t_2)} \simeq \sum_n \frac{1}{\sqrt{n!}} \int dx'_0 \int \frac{d^n \mathbf{k}'}{(2\pi)^n} e^{ix'_0 \sum_j k'_j} \times \mathcal{F}_n^*(\mathbf{k}') e^{+i \sum_j \epsilon(k'_j)(t_1+t_2)} \langle \mathbf{r}_4; \mathbf{k}' | \quad (24)$$

with $r_4 = x'_0 + v(k'_j)(t_1 + t_2)$. The ket side can be built progressively. $|\psi_1\rangle = U(t_1)M|0\rangle$ is given by Eq. (21). We are then interested in the scenario where M produces an extra WP at $q = 0$ on top of $|\psi_1\rangle$:

$$|\psi_2\rangle = M|\psi_1\rangle \simeq \sum_n \frac{1}{\sqrt{n!}} F_1(0) \int dx_0 \int dx_1 \int \frac{d^n \mathbf{k}}{(2\pi)^{n-1}} e^{-ix_0 \sum_j k_j} \times \mathcal{F}_n(\mathbf{k}) e^{-i \sum_j \epsilon(k_j)t_1} |(\mathbf{r}, x_1); (\mathbf{k}, 0)\rangle + \dots \quad (25)$$

The states can then be evolved semiclassically up to time $t_2 + t_1$. Along this evolution, any of the WPs produced at $t = 0$ crosses the trajectory of the $q = 0$ WP produced at $t = t_1$, the overall wavefunction acquires a phase given by the product of the scattering matrices for each crossing. We denote this phase as $\mathfrak{S}(x_0, x_1; \mathbf{k})$. Finally the ket side is given by $|\psi_3\rangle = MU(t_2)|\psi_2\rangle$. Here, as described in the main text, we consider the case where M annihilates the

$q = 0$ WP, thus producing

$$|\psi_3\rangle \simeq \sum_n \frac{|\mathcal{F}_1(0)|^2}{\sqrt{n!}} \int dx_1 \int dx_0 \int \frac{d^n \mathbf{k}}{(2\pi)^{n-1}} \\ \times e^{-ix_0 \sum_j k_j} \mathcal{F}_n(\mathbf{k}) e^{-i \sum_j \epsilon(k_j)(t_1+t_2)} |\mathbf{r}; \mathbf{k}\rangle \\ \times \mathfrak{S}(x_0, x_1; \mathbf{k}) + \dots, \quad (26)$$

with $r_j = x_0 + v(k_j)(t_1 + t_2)$.

Finally, we can take the overlap between the bra and ket $\langle \psi_4 | \psi_3 \rangle$. Comparing the expressions for the two we see that only the terms with $\|\mathbf{k} - \mathbf{k}'\| \lesssim \ell^{-1}$ and $|x_0 - x'_0| \lesssim \ell$ give a significant overlap. This gives an overall view of how to extend the semiclassical picture to the non-integrable case. The crucial point, however, remains that for any values of the other integration variables s.t. $\sum_j k_j \approx 0$ we have

$$\int dx_0 (\mathfrak{S}(x_0, x_1; \mathbf{k}) - 1) \propto (t_1 + t_2), \quad (27)$$

meaning that upon rescaling both times by some factor λ , the integral is also rescaled by λ . These considerations therefore lead us to the scaling form Eq. (4) also in non-integrable theories. A more detailed analysis will be presented in Ref. [37].

-
- [1] P. C. Martin, *Measurements and correlation functions* (CRC Press, 1968).
- [2] G. Giuliani and G. Vignale, *Quantum Theory of the Electron Liquid* (Cambridge University Press, 2005).
- [3] S. Mukamel, *Principles of nonlinear optical spectroscopy*, 6 (Oxford University Press on Demand, 1999).
- [4] Y. Wan and N. P. Armitage, *Phys. Rev. Lett.* **122**, 257401 (2019).
- [5] P. Jepsen *et al.*, *App. Phys. Lett.* **79**, 1291 (2001).
- [6] A. Cavalleri, C. Tóth, C. W. Siders, J. A. Squier, F. Ráksi, P. Forget, and J. C. Kieffer, *Phys. Rev. Lett.* **87**, 237401 (2001).
- [7] S. A. Lynch, P. T. Greenland, A. F. van der Meer, B. N. Murdin, C. R. Pidgeon, B. Redlich, N. Q. Vinh, and G. Aepli, in *35th International Conference on Infrared, Millimeter, and Terahertz Waves* (IEEE, 2010) pp. 1–2.
- [8] W. Kuehn, K. Reimann, M. Woerner, T. Elsaesser, and R. Hey, *J. Phys. Chem. B* **115**, 5448 (2011).
- [9] M. Woerner, W. Kuehn, P. Bown, K. Reimann, and T. Elsaesser, *New J. Phys.* **15**, 025039 (2013).
- [10] J. Lu, Y. Zhang, H. Y. Hwang, B. K. Ofori-Okai, S. Fleischer, and K. A. Nelson, *Proc. Natl. Acad. Sci.* **113**, 11800 (2016).
- [11] F. Mahmood, D. Chaudhuri, S. Gopalakrishnan, R. Nandkishore, and N. P. Armitage, *Nature Physics* **17**, 627 (2021).
- [12] D. Chaudhuri, D. Barbalas, R. Romero III, F. Mahmood, J. Liang, J. Jesudasan, P. Raychaudhuri, and N. P. Armitage, arXiv e-prints, arXiv:2204.04203 (2022), arXiv:2204.04203 [cond-mat.supr-con].
- [13] Z. Li, T. Tohyama, T. Iitaka, H. Su, and H. Zeng, arXiv e-prints, arXiv:2001.07839 (2020), arXiv:2001.07839 [cond-mat.mtrl-sci].
- [14] W. Choi, K. H. Lee, and Y. B. Kim, *Phys. Rev. Lett.* **124**, 117205 (2020).
- [15] M. Kanega, T. N. Ikeda, and M. Sato, *Phys. Rev. Research* **3**, L032024 (2021).
- [16] K. Shinada and R. Peters, arXiv e-prints, arXiv:2110.10496 (2021), arXiv:2110.10496 [cond-mat.str-el].
- [17] Y. Michishita and R. Peters, *Phys. Rev. B* **103**, 195133 (2021).
- [18] F. B. Kugler, S.-S. B. Lee, and J. von Delft, *Phys. Rev. X* **11**, 041006 (2021).
- [19] S.-S. B. Lee, F. B. Kugler, and J. von Delft, *Phys. Rev. X* **11**, 041007 (2021).
- [20] H. Watanabe and M. Oshikawa, *Phys. Rev. B* **102**, 165137 (2020).
- [21] H. Watanabe, Y. Liu, and M. Oshikawa, *Journal of Statistical Physics* **181**, 2050 (2020).
- [22] K. Takasan, M. Oshikawa, and H. Watanabe, arXiv e-prints, arXiv:2105.11378 (2021), arXiv:2105.11378 [cond-mat.mes-hall].
- [23] Y. Michishita and N. Nagaosa, arXiv e-prints, arXiv:2204.08365 (2022), arXiv:2204.08365 [cond-mat.str-el].
- [24] T. Morimoto, S. Zhong, J. Orenstein, and J. E. Moore, *Phys. Rev. B* **94**, 245121 (2016).
- [25] S. A. Parameswaran and S. Gopalakrishnan, *Phys. Rev. Lett.* **125**, 237601 (2020).
- [26] R. M. Nandkishore, W. Choi, and Y. B. Kim, *Phys. Rev. Research* **3**, 013254 (2021).
- [27] I. Sodemann and L. Fu, *Phys. Rev. Lett.* **115**, 216806 (2015).
- [28] D. E. Parker, T. Morimoto, J. Orenstein, and J. E. Moore, *Phys. Rev. B* **99**, 045121 (2019).
- [29] S. M. João and J. M. V. P. Lopes, *Journal of Physics: Condensed Matter* **32**, 125901 (2019).
- [30] I. Paul, arXiv e-prints, arXiv:2101.04136 (2021), arXiv:2101.04136 [cond-mat.str-el].
- [31] B. Doyon, *SciPost Physics* **5**, 54 (2018).
- [32] B. Doyon and J. Myers, *Annales Henri Poincaré* **21**, 255 (2019).
- [33] J. Myers, M. J. Bhaseen, R. J. Harris, and B. Doyon, *SciPost Phys.* **8**, 7 (2020).
- [34] Y. Tanikawa, K. Takasan, and H. Katsura, *Phys. Rev. B* **103**, L201120 (2021).
- [35] Y. Tanikawa and H. Katsura, *Phys. Rev. B* **104**, 205116 (2021).
- [36] M. Fava, S. Biswas, S. Gopalakrishnan, R. Vasseur, and S. A. Parameswaran, *Proceedings of the National Academy of Sciences* **118**, e2106945118 (2021), <https://www.pnas.org/doi/pdf/10.1073/pnas.2106945118>.
- [37] M. Fava, S. Gopalakrishnan, R. Vasseur, S. A. Parameswaran, and F. Essler, “Divergent nonlinear response in integrable systems,” (2022).
- [38] See, e.g. Appendix A of P. Calabrese, F. H. L. Essler, and M. Fagotti, *Journal of Statistical Mechanics: Theory and Experiment* **2012**, P07016 (2012).
- [39] F. H. L. Essler and R. M. Konik, *Phys. Rev. B* **78**, 100403 (2008).
- [40] F. H. L. Essler and R. M. Konik, *Journal of Statistical Mechanics: Theory and Experiment* **2009**, P09018 (2009).

- [41] B. Pozsgay and G. Takács, *Nuclear Physics B* **788**, 209 (2008).
- [42] B. Pozsgay and G. Takács, *Journal of Statistical Mechanics: Theory and Experiment* **2010** (2010).
- [43] P. Calabrese, F. H. L. Essler, and M. Fagotti, *Phys. Rev. Lett.* **106**, 227203 (2011).
- [44] D. Schuricht and F. H. L. Essler, *Journal of Statistical Mechanics: Theory and Experiment* **2012**, P04017 (2012).
- [45] F. H. L. Essler, S. Evangelisti, and M. Fagotti, *Phys. Rev. Lett.* **109**, 247206 (2012).
- [46] E. Granet, M. Fagotti, and F. H. L. Essler, *SciPost Phys.* **9**, 33 (2020).
- [47] A. I. Larkin and Y. N. Ovchinnikov, *Soviet Journal of Experimental and Theoretical Physics* **28**, 1200 (1969).
- [48] S. H. Shenker and D. Stanford, *Journal of High Energy Physics* **2014**, 1 (2014).
- [49] A. Kitaev, “Hidden correlations in the Hawking radiation and thermal noise,” talk at Fundamental Physics Prize Symposium (2015).
- [50] S. Sachdev and A. Young, *Physical review letters* **78**, 2220 (1997).
- [51] S. Sachdev, *Nuclear Physics B* **464**, 576 (1996).
- [52] H. Rieger and F. Iglói, *Phys. Rev. B* **84**, 165117 (2011).
- [53] B. Blass, H. Rieger, and F. Iglói, *EPL (Europhysics Letters)* **99**, 30004 (2012).
- [54] S. Evangelisti, *Journal of Statistical Mechanics: Theory and Experiment* **2013**, P04003 (2013).
- [55] M. Kormos and G. Zaránd, *Phys. Rev. E* **93**, 062101 (2016).
- [56] A. I. Bugrij, *Theoretical and Mathematical Physics* **127**, 528 (2001).
- [57] A. Bugrij and O. Lisovyy, *Physics Letters A* **319**, 390 (2003).
- [58] G. von Gehlen, N. Iorgov, S. Pakuliak, V. Shadura, and Y. Tykhyy, *Journal of Physics A: Mathematical and Theoretical* **41**, 095003 (2008).
- [59] N. Iorgov, V. Shadura, and Y. Tykhyy, *Journal of Statistical Mechanics: Theory and Experiment* **2011**, P02028 (2011).
- [60] H. Babujian, M. Karowski, and A. Tsvetik, *Nuclear Physics B* **917**, 122 (2017).
- [61] H. M. Babujian, M. Karowski, and A. M. Tsvetik, *Phys. Rev. B* **94**, 155156 (2016).
- [62] G. D. V. D. Vecchio and B. Doyon, *Journal of Statistical Mechanics: Theory and Experiment* **2022**, 053102 (2022).